

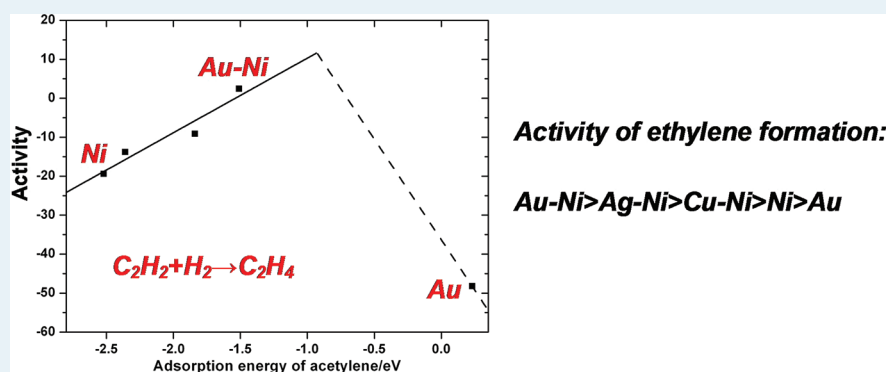
# Origin of the Increase of Activity and Selectivity of Nickel Doped by Au, Ag, and Cu for Acetylene Hydrogenation

Bo Yang,<sup>†</sup> Robbie Burch,<sup>†</sup> Christopher Hardacre,<sup>\*,†</sup> Gareth Headdock,<sup>‡</sup> and P. Hu<sup>\*,†</sup>

<sup>†</sup>School of Chemistry & Chemical Engineering, Queen's University, Belfast, BT9 5AG, U. K.

<sup>‡</sup>Johnson Matthey Catalysts, PO Box 1, Billingham, Teesside, TS23 1LB, U.K.

## Supporting Information



**ABSTRACT:** Activity and selectivity are both important issues in heterogeneous catalysis and recent experimental results have shown that Ni catalysts doped by gold exhibit high activity for the hydrogenation of acetylene with good selectivity of ethylene formation. To unravel the underlying mechanism for this observation, the general trend of activity and selectivity of Ni surfaces doped by Au, Ag, and Cu has been investigated using density functional theory calculations. Complete energy profiles from  $C_2H_2$  to  $C_2H_4$  on Ni(111), Au/Ni(111), Ag/Ni(111) and Cu/Ni(111) are obtained and their turnover frequencies (TOFs) are computed. The results show that acetylene adsorption on Ni catalyst is strong which leads to the low activity while the doping of Au, Ag, and Cu on the Ni catalyst weakens the acetylene adsorption, giving rise to the increase of activity. The selectivity of ethylene formation is also quantified by using the energy difference between the hydrogenation barriers and the absolute value of the adsorption energies of ethylene. It is found that the selectivity of ethylene formation increases by doping Au and Ag, while those of Cu/Ni and Ni are similar.

**KEYWORDS:** DFT, selective hydrogenation, activity, selectivity, acetylene, ethylene, Ni, Au, Ag, Cu

## INTRODUCTION

The selective removal of acetylene from ethylene feeds is crucial in the olefin industry as acetylene acts not only as an impurity in the ethylene feed, but also as a poison to the catalyst used for subsequent polymerization of the ethylene.<sup>1,2</sup> The most widely used method to remove acetylene in ethylene feed in the industry is to selectively hydrogenate acetylene to ethylene which gives rise to the double benefit of lowering the concentration of acetylene while increasing the production of the desired ethylene. However, as ethylene is also an unsaturated hydrocarbon and the possibility of its hydrogenation to produce saturated product ethane still exists, the catalysts employed should be highly selective to ensure that no ethane is formed. Moreover, as the concentration of acetylene needs to be as low as only a few ppm to minimize the effect on the polymerization of ethylene, the catalysts to remove acetylene should also be highly active.

Palladium has long been identified to have both high selectivity and high activity for the acetylene hydrogenation and Pd-based catalysts have played a leading role in the industry.

Addition of inert metals like Au, Ag and Cu have also been used to improve the performance of Pd for the reaction.<sup>3</sup> Nickel catalysts, which show high selectivity to ethylene, have also been used in this reaction. In fact, the crucial factor affecting the selectivity of acetylene hydrogenation to ethylene is thought to be the difference between the adsorption energy and the hydrogenation barrier of ethylene on the catalyst surface.<sup>4,5</sup> This is reasonable since the ethylene on the surface will either be hydrogenated or desorb from the surface; the possibility of the hydrogenation can be measured by the hydrogenation barrier while the chance of desorption of ethylene can be estimated from the adsorption energy. When the adsorption energy of ethylene is lower than that of the hydrogenation barrier, ethylene will prefer to desorb from the catalyst surface. Using density functional calculations, Nørskov and co-workers used these rules to design a highly selective catalyst based on a

**Received:** December 21, 2011

**Revised:** April 14, 2012

**Published:** April 18, 2012

bimetallic NiZn catalyst which shows low ethane formation during the hydrogenation.<sup>4</sup> However, the temperature used for those Ni-based catalysts was up to 523 K,<sup>6</sup> which is much higher than the temperature desired for industrial utilization, and higher than that used for Pd-based catalysts, which is commonly used below 373 K. This is consistent with the fact that Ni has been identified to be less active than Pd for this reaction. Recently, an interesting result was observed by Nikolaev et al. They reported that the conversion of acetylene on Ni–Au bimetallic catalysts was higher by about an order of magnitude than that on catalysts based on individual gold or nickel.<sup>7,8</sup> It is not surprising that the activity of bimetallic catalysts is higher than pure gold catalyst as gold has long been recognized as the most inert transition metal and shows low activity for the hydrogenation reactions.<sup>9–11</sup> However, the higher activity of Ni–Au catalysts than pure Ni is unexpected. Furthermore, the selectivity of all the Ni–Au catalysts tested for this reaction over the entire test temperature was found to be  $\geq 99.99\%$ .

In this work, we first investigated the determining factor for the low activity of Ni for the selective acetylene hydrogenation. Then the Ni surface alloyed with Au was studied to unravel the origin of the activation of Ni by gold. The general trend of Ni(111) and M/Ni(111) (M = Au, Ag, and Cu) was also studied in this work.

## ■ COMPUTATIONAL DETAILS

The density functional calculations shown in this work were performed with the Vienna Ab-initio Simulation Package (VASP)<sup>12–15</sup> in slab models. The exchange-correlation functional PW91<sup>16</sup> was used to calculate the electronic structure with generalized gradient approximation (GGA). The projector augmented wave (PAW) method was employed to describe the interaction between atomic cores and electrons.<sup>17,18</sup> For Ni(111), Au/Ni(111), Ag/Ni(111) and Cu/Ni(111) surfaces, four layer  $2 \times 2$  slabs with the upmost two layers relaxed during optimization were used to model the adsorption and reaction processes. The different surface alloys were modeled with the substitution of surface Ni atoms with Cu, Ag and Au atoms. It should also be noted that the main focus of the present work is to understand the promotion effects of Cu, Ag and Au on the reactivity/selectivity of Ni for acetylene hydrogenation. Therefore, a basic model system was used in order to obtain clear trends which did not include the complicating factors of the formation of carbide or hydride during the hydrogenation. Both are likely to form during the reaction and perturb the mechanism of acetylene hydrogenation on Ni;<sup>6,19–21</sup> however, this is thought to be secondary compared with the main effect of the additives on the Ni. A  $5 \times 5 \times 1$  *k*-point sampling in the surface Brillouin zone was used in the calculations. The vacuum was set to be more than 12 Å to ensure that there is little interaction between slabs. Spin polarization was considered for the calculations of all the models. An energy cutoff of 500 eV and the converge criteria of the force on each relaxed atoms below 0.05 eV/Å were used in this work. The transition states were located with a constrained minimization method.<sup>22–24</sup> The adsorption energies are defined as follows:

$$E_{\text{ad}} = E_{\text{total}} - (E_{\text{g}} + E_{\text{slab}}) \quad (1)$$

$E_{\text{total}}$  is the energy of the system after adsorption,  $E_{\text{g}}$  denotes the energy of the gas phase adsorbent, and  $E_{\text{slab}}$  is the energy of slab.

The doped Ni(111) was modeled with the substitution of surface Ni atom by Au, Ag and Cu atoms, respectively, as shown in Figure 1.

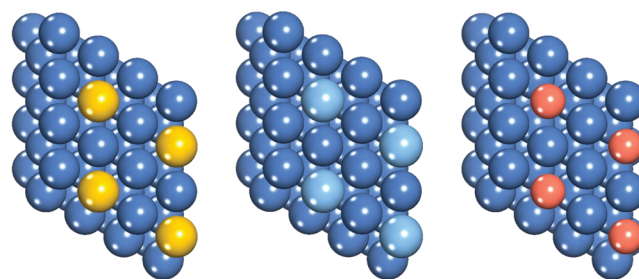


**Figure 1.** Structures of surface alloyed Au/Ni(111), Ag/Ni(111), and Cu/Ni(111) surfaces (from left to right). The dark blue, yellow, light blue and red balls denote the Ni, Au, and Cu atoms, respectively. This definition is used through out the paper.

## ■ RESULTS AND DISCUSSION

The adsorption of acetylene on all the surfaces was first calculated to obtain the most stable system. The adsorption structures are shown in Figure 2 and the adsorption energies are listed in Table 1. It can be seen that the adsorption energies of acetylene on these surfaces follow the order Ni(111) > Cu/Ni(111) > Ag/Ni(111) > Au/Ni(111), which is consistent with the order of the reactivity for the pure Cu, Ag and Au systems. The adsorption geometry of acetylene was also found to be slightly different on each surface. On Ni(111) and Cu/Ni(111), the acetylene sits on four metal atoms, which is consistent with previous study of the adsorption of acetylene on Ni(111) surface.<sup>25,26</sup> In contrast, acetylene adsorbs on three Ni atoms on both Au/Ni(111) and Ag/Ni(111), which is the same as that reported on Pd(111).<sup>25–31</sup> It is also obvious that the adsorption energies of the former Ni(111) and Cu/Ni(111) structures are much higher than the Au/Ni(111) and Ag/Ni(111) structures. We will show that the adsorption structures and the energies of acetylene on these surfaces significantly influence the hydrogenation activity later.

The transition states of acetylene hydrogenation on these surfaces were located, the structures of which are also shown in Figure 1, and the reaction barriers are listed in Table 1. It can be seen that similar to the adsorption structures and the energies of acetylene hydrogenation on these surfaces, the transition state structures and the reaction barriers also fall into two types. The hydrogen atom in each transition state of acetylene hydrogenation on Ni(111) and Cu/Ni(111) sits on two Ni atoms while on Ag/Ni(111) and Au/Ni(111) it sits on only one Ni atom. The latter is also found on Pd(111).<sup>29</sup> Furthermore, the reaction barriers of acetylene hydrogenation on Ni(111) and Cu/Ni(111) are considerably higher than those on either Ag/Ni(111) and Au/Ni(111) surfaces. In contrast, the adsorption geometry of the product from the first hydrogenation, that is,  $\text{C}_2\text{H}_2 + \text{H} \rightarrow \text{C}_2\text{H}_3$ , shown in Supporting Information Figure S2, was found to adsorb at the hollow site of three Ni atoms on all of the surfaces studied and the calculated hydrogenation barriers of  $\text{C}_2\text{H}_3$  on all of the surfaces were found to be similar as well as the transition state structures (see Table 1 and Supporting Information Figure S2). Differences were found in the reaction energies of  $\text{C}_2\text{H}_2 + \text{H} \rightarrow \text{C}_2\text{H}_3$  with values of 0.71, 0.51, 0.35, and 0.11 eV on the

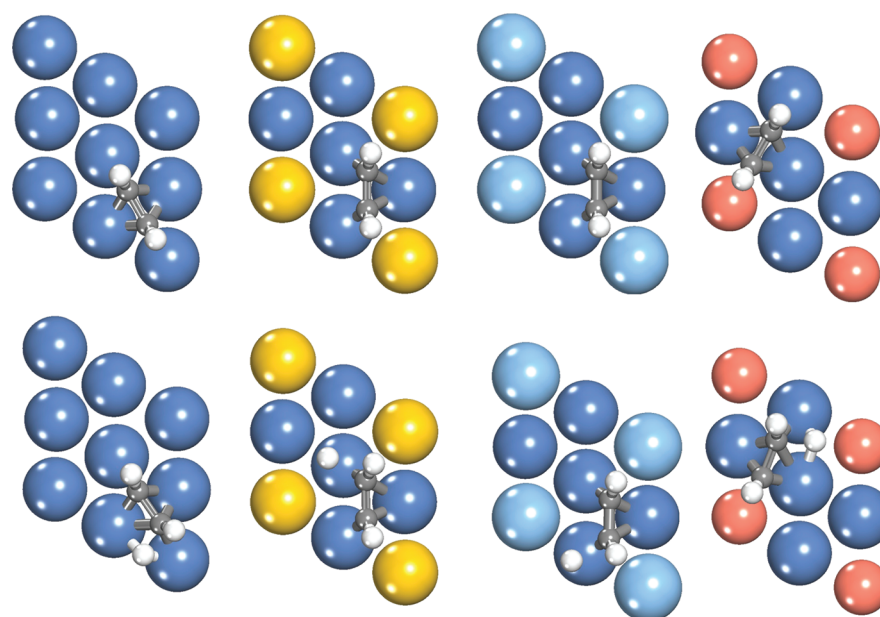


**Figure 2.** Adsorption (above) and transition state (below) structures of acetylene and acetylene hydrogenation on Ni(111), Au/Ni(111), Ag/Ni(111) and Cu/Ni(111) surfaces (from left to right). The gray and white balls denote the carbon and hydrogen atoms, respectively.

**Table 1.** Adsorption Energies of Acetylene ( $E_{\text{ad,C}_2\text{H}_2}$ ) on Ni(111), Au/Ni(111), Ag/Ni(111), and Cu/Ni(111) Surfaces, Which Are Calculated Using Eq 1<sup>a</sup>

	Ni(111)	Au/Ni(111)	Ag/Ni(111)	Cu/Ni(111)
$E_{\text{ad,C}_2\text{H}_2}$ (eV)	-2.52	-1.51	-1.84	-2.36
$E_{\text{a,C}_2\text{H}_2}$ (eV)	1.04	0.82	0.93	1.08
$E_{\text{a,C}_2\text{H}_3}$ (eV)	0.77	0.69	0.82	0.80

<sup>a</sup>This table also shows the hydrogenation barriers of  $\text{C}_2\text{H}_2$  ( $E_{\text{a,C}_2\text{H}_2}$ ) and  $\text{C}_2\text{H}_3$  ( $E_{\text{a,C}_2\text{H}_3}$ ) on these surfaces.

Ni(111), Cu/Ni(111), Ag/Ni(111), and Au/Ni(111) surfaces, respectively. The calculations herein are consistent with the Brønsted–Evans–Polanyi (BEP) relationship which indicates that the reaction barriers increase with the increase of reaction energies for each elementary step on each surface (Supporting Information Figure S4). To further understand why the first hydrogenation barriers of acetylene, that is, the reaction barriers of  $\text{C}_2\text{H}_2 + \text{H} \rightarrow \text{C}_2\text{H}_3$ , on Au/Ni(111) and Ag/Ni(111) are lower than those on Ni(111) and Cu/Ni(111), we used energy decomposition method<sup>32,33</sup> to analyze the reaction barriers (the details of the energy decomposition method are shown in Supporting Information). It can be seen from Supporting Information Table S1 that the main difference lies in the different interaction energies between  $\text{C}_2\text{H}_2$  and H at the transition states. Furthermore, a linear relationship between the hydrogenation barriers and the interaction energy between  $\text{C}_2\text{H}_2$  and H was also found, shown in Supporting Information Figure S5.

The energy profiles containing the entropic effects from gas phase acetylene and hydrogen to the gas phase ethylene on the four surfaces are shown in Figure 3. The details of the calculation of the free energy changes and the adsorption and desorption barriers are shown in the Supporting Information. From these results, we can compare the different activities of four surfaces for the hydrogenation of acetylene to the ethylene.

Here, the energetic span theory is employed to obtain the turnover frequencies (TOFs).<sup>34–37</sup> According to this theory, TOF can be written as

$$\text{TOF} \approx \frac{k_{\text{B}}T}{h} e^{-E_{\text{a}}^{\text{eff}}/RT} \quad (2)$$

where  $E_{\text{a}}^{\text{eff}}$  is the effective reaction barrier, which will be discussed below. Hence, the TOF will only be related to the effective reaction barrier at the same temperature. In the energetic span theory, the effective reaction barriers are not the reaction barriers of the rate-determining steps but the energy differences between two rate-determining states in the whole energy profiles. The details of how to determine the effective barriers are shown in the Supporting Information and can also be found in the references.<sup>34–37</sup> As the range of TOFs is wide, from eq 2, one can write:

$$\ln(\text{TOF}) \approx \ln\left(\frac{k_{\text{B}}T}{h}\right) + \frac{-E_{\text{a}}^{\text{eff}}}{RT} \quad (3)$$

The estimated  $\ln(\text{TOF})$  was plotted against the adsorption energies of acetylene on Ni(111), Au/Ni(111), Ag/Ni(111), and Cu/Ni(111) surfaces and is shown in Figure 4. It can be seen that there is a linear relationship between them and shows a reasonable correlation ( $R^2 = 0.89$ ) with the data. For example, acetylene adsorbs on Ni(111) most strongly while the hydrogenation activity is the lowest on this surface. This suggests that the low activity of Ni for acetylene hydrogenation is caused by the strong adsorption of acetylene. From this plot, the effect of doping of Au, Ag, and Cu can be readily understood which increases the activity of the pure Ni catalyst. In these systems, the relationship between the activities and the adsorption energies of acetylene may all lie on the strong adsorption side of the volcano curve. Therefore, the more inert the dopant is, the more active the surface will be. To confirm this, we calculated the  $\ln(\text{TOF})$  of acetylene hydrogenation with respect to the adsorption energy of acetylene on Au(111) in Figure 4. It should be noted that the effective barrier of acetylene

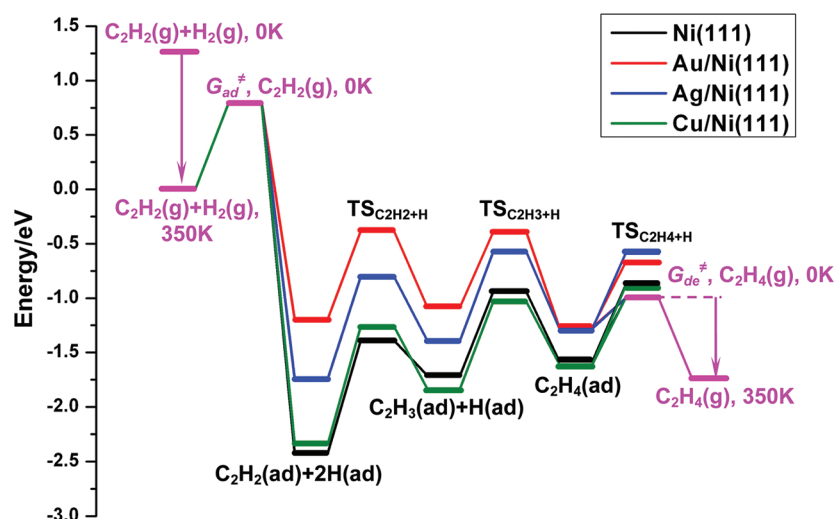


**Figure 3.** Energy profiles of  $C_2H_2$  hydrogenation to  $C_2H_4$  and  $C_2H_4$  hydrogenation under the standard pressure on Ni(111), Au/Ni(111), Ag/Ni(111), and Cu/Ni(111) surfaces. (ad) stands for the adsorption state while (g) stands for the gas phase state. For the adsorption and desorption, the entropic effects are considered.  $G_{ad}^\ddagger$  and  $G_{de}^\ddagger$  are the adsorption and desorption transition states of the reactant and the product, respectively, which are estimated from the entropy changes of  $C_2H_2$  and  $C_2H_4$ . The contribution of the entropy term to the free energies of each gas phase are  $\Delta\mu(0.1 \text{ bar } C_2H_2 + 1 \text{ bar } H_2, 350 \text{ K}) = 1.26 \text{ eV}$  and  $\Delta\mu(8.9 \text{ bar } C_2H_4, 350 \text{ K}) = 0.73 \text{ eV}$ . The transition state energies of  $C_2H_4$  hydrogenation are obtained by using  $E_{(C_2H_4(ad))} + E_{a,C_2H_4}$  for clarity.

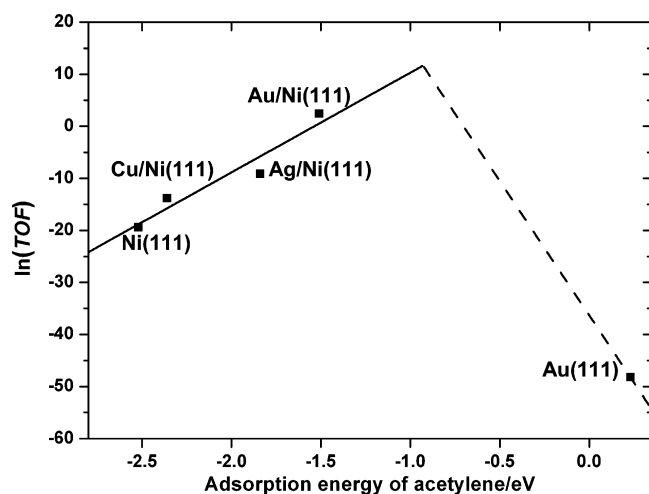


**Figure 4.** Volcano type of curve in which  $\ln(\text{TOF})$  is plotted as a function of the adsorption energies of acetylene on Ni(111), Au/Ni(111), Ag/Ni(111), Cu/Ni(111), and Au(111) surfaces. The relative effective barriers for acetylene hydrogenation on Ni(111), Au/Ni(111), Ag/Ni(111), and Cu/Ni(111) surfaces are shown in the main text. The hydrogenation of acetylene on Au(111) surface are calculated using the same method with those for other surfaces (the effective barrier is 2.35 eV). The weak adsorption side of the volcano curve is approximately illustrated by the dashed line.

hydrogenation on Au(111) was obtained using the sequential addition mechanism<sup>38,39</sup> that is the same as that on Ni based surfaces. It is obvious now that the low activity of pure Ni and Au has different origins; acetylene binds too strong on Ni while on Au the binding is too weak. Therefore, when both two metals are mixed to form an alloy catalyst, the adsorption of acetylene will be stronger than pure Au but weaker than pure Ni, which will effectively increase the activity of the surface. Our calculations are consistent with the experimental results previously reported for a Ni–Cu catalyst which was structurally promoted by Fe.<sup>40,41</sup> This catalyst only showed reasonable activity at high temperatures (>423 K) while a Ni modified by

**Table 2.** Adsorption Energies ( $E_{ad,e}$ ) and Hydrogenation Barriers ( $E_a$ ) of Ethylene on Several Model Flat Surfaces, Also Shown Are  $\Delta E$  Defined in Eq 4

	Ni(111)	Au–Ni(111)	Ag–Ni(111)	Cu–Ni(111)
$E_{ad,e}$ (eV)	−0.58	−0.27	−0.28	−0.61
$E_a$ (eV)	0.70	0.60	0.69	0.72
$\Delta E$ (eV)	0.12	0.33	0.41	0.11

Au showed acetylene conversion at much lower temperatures (79% at 293 K).<sup>7</sup> It should be noted that the activity of Au/Ni(111) is much higher than that of Ni(111) from our calculations and the activity difference is higher than the experimental work. We believe that it may be a result of the coverage effect not being properly included in the TOF estimations.

The selectivity of the hydrogenation of acetylene to ethylene was also investigated in this work. The selectivity of ethylene can be estimated by comparing the difference between the hydrogenation barrier and the desorption barrier of ethylene. In our previous work, several models were employed to measure the adsorption or desorption barriers of adsorbents over the catalyst surfaces.<sup>42</sup> It was found that desorption barriers were, in general, lower than the absolute value of the adsorption energies of the adsorbents. As the exact barriers are difficult to be measured, herein, the absolute value of the adsorption energies was used as a measure for the desorption barrier in order to obtain a general trend of all the surfaces, which is similar to our previous work on the selectivity of acrolein hydrogenation over both Pt and Au surfaces.<sup>38</sup> Thus an ideal catalyst should have a high hydrogenation barrier for ethylene and a low adsorption energy. We hereby define

$$\Delta E = E_a - |E_{ad}| \quad (4)$$

where  $E_a$  is the hydrogenation barrier of ethylene and  $E_{ad}$  is the adsorption energy. Table 2 lists the adsorption energies and hydrogenation barriers of ethylene on Ni(111), Au/Ni(111), Ag/Ni(111), and Cu/Ni(111) surfaces, the structures of which are shown in Supporting Information Figure S3. For the second

hydrogenation of  $C_2H_2$ , that is,  $C_2H_2 + H \rightarrow C_2H_3$ , there is also another possible hydrogenation product,  $CH_3CH$ . We calculated the energetics from  $CH_2CH$  to  $CH_3CH_2$  through the  $CH_3CH$  formation pathway on Ni(111), which is shown in Supporting Information Figure S6. One can see that the energetics of the formation of  $CH_3CH$  is just comparable with the pathway of  $CH_2CH_2$  formation and the difference lie in the error of DFT calculations, which is similar to previous results of acetylene hydrogenation on Pd(111).<sup>20,31</sup> However, the desorption pathway of ethylene from the Ni(111) surface is the favored one among the three pathways. It can be seen from Table 2 that Ag/Ni(111) has the highest  $\Delta E$  and then Au/Ni(111), and both are much higher than those of Ni(111) and Cu/Ni(111) surfaces, which means that the selectivity of acetylene hydrogenation to ethylene is highest on Ag/Ni(111) and then on Au/Ni(111). We found that, although the adsorption energies of ethylene on Ag/Ni(111) and Au/Ni(111) are found to be very similar, the H adsorption on Ag/Ni (−0.58 eV) is higher than that on Au/Ni (−0.47 eV). Thus, a higher energy is required to activate the H from the initial adsorption state to the transition state resulting in the higher barrier for the hydrogenation reaction on Ag/Ni(111). Furthermore, we found that the difference between the hydrogenation barriers of ethylene on Ag/Ni(111) and Au/Ni(111) is 0.09 eV, and is very similar with the difference between the adsorption energies of H on each surface (0.11 eV), which further supports the suggestion above. Moreover, the same trend was also found comparing the adsorption energies of H (−0.58 eV and −0.61 eV) and the hydrogenation barriers of ethylene (0.70 and 0.72 eV) on Ni(111) and Cu/Ni(111) surfaces, respectively. This link is also found comparing Ag/Ni(111) and Ni(111) wherein both the hydrogen adsorption energies and the hydrogenation barriers for ethylene are similar. However, all the  $\Delta E$  values in Table 2 are positive which means the desorption of ethylene is preferred on all the surfaces and ethylene can be selectively formed in these systems. This result provides a good explanation for the high selectivity of ethylene observed in the experiments.<sup>7,8,40</sup>

## CONCLUSIONS

In conclusion, the crucial problem of Ni for acetylene hydrogenation has been identified to be the high adsorption energy of acetylene with the help of density functional theory calculations in this work. The doping of inert metals such as Au, Ag and Cu reduces the adsorption energy and thus leads to an increase in activity. The activity of bimetallic catalysts is found to follow the order of Au–Ni > Ag–Ni > Cu–Ni and they lie in the strong adsorption side of the volcano curve of acetylene hydrogenation. The selectivity of ethylene formation on the bimetallic surfaces, Au/Ni(111) and Ag/Ni(111) are also found to increase compared with pure Ni, although those of Cu/Ni and Ni are very similar. These results are in good agreement with the reported experimental results.

## ASSOCIATED CONTENT

### Supporting Information

Structures and detailed analyses of the effective barriers. This information is available free of charge via the Internet at <http://pubs.acs.org/>.

## AUTHOR INFORMATION

### Corresponding Author

\*E-mail: [c.hardacre@qub.ac.uk](mailto:c.hardacre@qub.ac.uk) (C.H.); [p.hu@qub.ac.uk](mailto:p.hu@qub.ac.uk) (P.H.).

## Notes

The authors declare no competing financial interest.

## ACKNOWLEDGMENTS

This work is financially supported by EPSRC and Johnson Matthey through the CASTech programme. The authors thank The Queen's University of Belfast for computing time. B.Y. also acknowledges the financial support of Dorothy Hodgkin Postgraduate Award (DHPA) studentship jointly funded by EPSRC and Johnson Matthey.

## REFERENCES

- (1) Borodziński, A.; Bond, G. C. *Catal. Rev.—Sci. Eng.* **2006**, *48*, 91.
- (2) Borodziński, A.; Bond, G. C. *Catal. Rev.—Sci. Eng.* **2008**, *50*, 379.
- (3) López, N.; Vargas-Fuentes, C. *Chem. Commun.* **2012**, *48*, 1379.
- (4) Studdt, F.; Abild-Pedersen, F.; Bligaard, T.; Sørensen, R. Z.; Christensen, C. H.; Nørskov, J. K. *Science* **2008**, *320*, 1320.
- (5) Studdt, F.; Abild-Pedersen, F.; Bligaard, T.; Sørensen, R. Z.; Christensen, C. H.; Nørskov, J. K. *Angew. Chem., Int. Ed.* **2008**, *47*, 9299.
- (6) Bridier, B.; López, N.; Pérez-Ramírez, J. J. *Catal.* **2010**, *269*, 80.
- (7) Nikolaev, S. A.; Smirnov, V. V.; Vasil'kov, A. Y.; Podshibikhin, V. L. *Kinet. Catal.* **2010**, *51*, 375.
- (8) Nikolaev, S. A.; Smirnov, V. V. *Catal. Today* **2009**, *147*, S336.
- (9) Hammer, B.; Nørskov, J. K. *Nature* **1995**, *376*, 238.
- (10) Jia, J. F.; Haraki, K.; Kondo, J. N.; Domen, K.; Tamaru, K. *J. Phys. Chem. B* **2000**, *104*, 11153.
- (11) Segura, Y.; López, N.; Pérez-Ramírez, J. J. *Catal.* **2007**, *247*, 383.
- (12) Kresse, G.; Hafner, J. *Phys. Rev. B* **1993**, *47*, 558.
- (13) Kresse, G.; Hafner, J. *Phys. Rev. B* **1994**, *49*, 14251.
- (14) Kresse, G.; Furthmüller, J. *Comput. Mater. Sci.* **1996**, *6*, 15.
- (15) Kresse, G.; Furthmüller, J. *Phys. Rev. B* **1996**, *54*, 11169.
- (16) Perdew, J. P.; Wang, Y. *Phys. Rev. B* **1992**, *45*, 13244.
- (17) Blöchl, P. E. *Phys. Rev. B* **1994**, *50*, 17953.
- (18) Kresse, G.; Joubert, D. *Phys. Rev. B* **1999**, *59*, 1758.
- (19) Sautet, P.; Cinquini, F. *ChemCatChem* **2010**, *2*, 636.
- (20) García-Mota, M.; Bridier, B.; Pérez-Ramírez, J.; López, N. *J. Catal.* **2010**, *273*, 92.
- (21) Bridier, B.; López, N.; Pérez-Ramírez, J. *Dalton Trans.* **2010**, *39*, 8412.
- (22) Alavi, A.; Hu, P.; Deutsch, T.; Silvestrelli, P. L.; Hutter, J. *Phys. Rev. Lett.* **1998**, *80*, 3650.
- (23) Liu, Z. P.; Hu, P. *J. Am. Chem. Soc.* **2003**, *125*, 1958.
- (24) Michaelides, A.; Liu, Z. P.; Zhang, C. J.; Alavi, A.; King, D. A.; Hu, P. *J. Am. Chem. Soc.* **2003**, *125*, 3704.
- (25) Medlin, J. W.; Allendorf, M. D. *J. Phys. Chem. B* **2003**, *107*, 217.
- (26) Basaran, D.; Aleksandrov, H. A.; Chen, Z. X.; Zhao, Z. J.; Rösch, N. *J. Mol. Catal. A* **2011**, *344*, 37.
- (27) Dunphy, J. C.; Rose, M.; Behler, S.; Ogletree, D. F.; Salmeron, M.; Sautet, P. *Phys. Rev. B* **1998**, *57*, R12705.
- (28) Mittendorfer, F.; Thomazeau, C.; Raybaud, P.; Toulhoat, H. *J. Phys. Chem. B* **2003**, *107*, 12287.
- (29) Sheth, P. A.; Neurock, M.; Smith, C. M. *J. Phys. Chem. B* **2003**, *107*, 2009.
- (30) Sheth, P. A.; Neurock, M.; Smith, C. M. *J. Phys. Chem. B* **2005**, *109*, 12449.
- (31) Chen, Z. X.; Aleksandrov, H. A.; Basaran, D.; Rösch, N. *J. Phys. Chem. C* **2010**, *114*, 17683.
- (32) Liu, Z. P.; Hu, P. *J. Chem. Phys.* **2001**, *114*, 8244.
- (33) Liu, Z. P.; Hu, P. *J. Chem. Phys.* **2001**, *115*, 4977.
- (34) Kozuch, S.; Shaik, S. *J. Am. Chem. Soc.* **2006**, *128*, 3355.
- (35) Kozuch, S.; Shaik, S. *Acc. Chem. Res.* **2010**, *44*, 101.
- (36) Kozuch, S.; Martin, J. M. L. *ACS Catal.* **2011**, *1*, 246.
- (37) Kozuch, S.; Martin, J. M. L. *Chem. Commun.* **2011**, *47*, 4935.
- (38) Yang, B.; Wang, D.; Gong, X.-Q.; Hu, P. *Phys. Chem. Chem. Phys.* **2011**, *13*, 21146.
- (39) Yang, B.; Cao, X.-M.; Gong, X.-Q.; Hu, P. *Phys. Chem. Chem. Phys.* **2012**, *14*, 3741.

- (40) Bridier, B.; Pérez-Ramírez, J. *J. Am. Chem. Soc.* **2010**, *132*, 4321.
- (41) Bridier, B.; Pérez-Ramírez, J.; Knop-Gericke, A.; Schlögl, R.; Teschner, D. *Chem. Sci.* **2011**, *2*, 1379.
- (42) Cao, X.-M.; Burch, R.; Hardacre, C.; Hu, P. *Catal. Today* **2011**, *165*, 71.